*Asian Journal of Environment and Disaster Management*
Vol. 3, No. 2 (2011) 229–242

doi:10.3850/S1793924011000770

# Identifying Shape Characteristics of Streamflow Hydrograph and Its Components

Chun-Dan Cheng[1,2,a], Shin-Jen Cheng[3,*], Jet-Chau Wen[1,2,4] and Ju-Huang Lee[5]

[1]*Graduate School of Engineering Science and Technology, National Yunlin University of Science and Technology, Douliu, Yunlin 640, Taiwan*
[2]*Research Center for Soil & Water Resources and Natural Disaster Prevention, National Yunlin University of Science & Technology, 123, Section 3, University Road, Douliu City, Yunlin County 640, Taiwan, R.O.C. E-mail: [a]g9510835@yuntech.edu.tw*
[3]*Department of Leisure and Recreation Management, Taiwan Shoufu University, 168, Nan-shih Li, Madou, 721, Tainan, Taiwan Taiwan. E-mail: sjcheng@tsu.edu.tw*
[4]*Department and Graduate School of Safety, Health and Environmental Engineering, National Yunlin University of Science and Technology, Douliou, Yunlin 640, Taiwan. E-mail: wenjc@yuntech.edu*
[5]*Hydrology & Technology Department of Water Resources Agency, Ministry of Economic Affairs of Republic of China, 9-12F., No. 41-3, Sec. 3, Xinyi Rd., Da'an Disrict., Taipei City 106, Taiwan, R.O.C. E-mail: rhlee@wra.gov.tw*

This study investigates the characteristics of hydrograph components based on flood disaster mitigation. Component hydrographs were modeled by a model of three serial tanks with one parallel tank. Mean rainfall was calculated using the block Kriging method. The seven parameters were calibrated using the shuffled complex evolution optimal algorithm and 38 events. Based on the analytical results, the findings were obtained: (1) For single-peak events, times to peak of hydrograph components are an increasing power correlation corresponding to peak time of rainfall; (2) The peak discharges of hydrograph components are linearly proportional to that of total runoff; the ratio for quick runoff is approximately 83% and 17% for the slow runoff; and (3) Relationships of total discharges also have direct ratios between hydrograph components and observed total runoffs; a quick runoff is 52% and 27% for a slow runoff. The remaining discharge is baseflow.

*Keywords*: Block Kriging; linear reservoir; streamflow components; hydrograph shape.

## 1. Introduction

In the past, many hydrologists were interested in developments of conceptual rainfall-runoff models. Generally, approximations of the convolution integral with unit hydrograph/instantaneous unit hydrograph (UH/IUH) are conveniently used to derive conceptual models for generating outlet-runoffs of a watershed. These models derived from the convolution integral are generally known as

*Corresponding author.

UH-based modeling. These derivations with specific parameters are the Nash model,[1] Clark IUH,[2] geomorphologic (IUH),[3] the distributed parallel model,[4] and subwatershed divisions.[5] Rainfall-runoff processes[6,7] have been modeled with IUH. Furthermore, changes of hydrograph characteristics on an urbanized watershed were also evaluated by identifying the relationships between IUH parameters and urbanization variables.[8–12]

Basically, essential materials of the UH-based models (e.g. Nash model) usually are recordings of rainfall and streamflow. Applying these models based on the IUH theory involves determining both the effective rainfall and the baseflow of a rainfall-runoff event in advance. Various works have addressed the effects of different methods for estimating rainfall excess and baseflow on the accuracy of modeling surface runoff.[8] Prior to IHACRES[13,14] and TANK,[15–18] hydrological modeling was not to generate total streamflow by a linear convolution with the specific input-output structures.

The assumptions of IUH like Nash's type linear reservoirs were preserved for the model used in this study, i.e., a uniform spatial distribution of rainfall and the principle of linear superposition. The model structure is serial cascades of three linear reservoirs and with one in parallel. Each linear reservoir has an exponential expression derived from the equation of continuity and convolution integral. These exponential expressions were used to illustrate storage statuses of the linear reservoirs during rainfall-runoff processes. Generating hydrograph components in a specific river during a storm is the first application of the proposed model. Then, the causal relationships among rainfall, total runoff observations, and generated runoff components were also discussed. The block Kriging method was used to estimate the mean rainfall as input for the model. Model parameters were acquired through an optimization approach. Three evaluated criteria were used to compare simulations and observations of total runoff hydrographs. The representative parameters are proportional to the magnitudes of the open holes and were used to determine surface, rapid subsurface, delayed subsurface and groundwater runoffs. Finally, hydrograph components (quick and slow flows) of the research watershed-outlet and their characteristics relating to observations of rainfall and total runoff were discussed and completed.

## 2. The Block Kriging Method

The block Kriging method was used to estimate hourly spatially uniform rainfall over the whole watershed. The Kriging method is theoretically better than the Thiessen method because Kriging has a spatial structure (i.e., semivariogram), while Thiessen has a lesser ability to represent the spatial structure of rainfall.

### 2.1. Climatological mean semivariogram

A basic semivariogram called the scaled climatological mean semivariogram was proposed[19] and established through dimensionless rainfall data on a project basin.[20] The relationship between the hourly experimental semivariogram and the scaled climatological mean semivariogram is shown below:

$$\gamma\left(t, h_{ij}\right) = \omega(t)\gamma_d^*\left(h_{ij}, a\right) = s^2(t)\gamma_d^*\left(h_{ij}, a\right) \tag{1}$$

where $\omega(t)$ denotes the sill of the semivariogram for time period $t$ ($mm^2$) and is time-variant; $a$ represents the range of the scaled climatological mean semivariogram (m) and is time-invariant; and $s(t)$ denotes the standard deviation of rainfall of all raingauges for time period $t$ (mm). The basic semivariogram is expressed as

$$\gamma_d^*(h_{ij}, a) = \frac{1}{2T}\sum_{t=1}^{T}\left\{\left[\frac{p(t, x_i) - p(t, x_j)}{s(t)}\right]^2\right\} \tag{2}$$

The basic experimental semivariogram can be calculated by using Eq. (2). Because this semivariogram is derived from discontinuous point-observations, it is not spatially continuous. A realistic application is to use a semivariogram model (Eq. (3)), named the power model, to obtain spatial continuity of rainfall variations.

$$\gamma_d^*(h_{ij}, a) = \omega_0 h_{ij}^a, \quad a < 2 \tag{3}$$

where $\omega_0$ denotes the sill of the scaled climatological mean semivariogram ($mm^2$) and is a constant of approximately one except for the power model.

### 2.2. Block Kriging system

The block Kriging method obtains optimal weights that are obtained from the Kriging system by assuming a given spatial structure of rainfall. The estimated area $V$ must be divided into $M$ grids before calculating the hourly mean rainfall of storm events over the watershed by applying Eq. (4) and Eq. (5).

$$\begin{cases} \sum_{j=1}^{n} \lambda_j \gamma(x_i, x_j) + \mu = \bar{\gamma}(V_m, x_i), \quad i = 1, 2, \ldots, n \\ \sum_{i=1}^{n} \lambda_i = 1 \end{cases} \tag{4}$$

$$\sigma_K^2 = \sum_{i=1}^{n} \lambda_i \bar{\gamma}(V, x_i) + \mu \tag{5}$$

where $\gamma(x_i, x_j)$ is the semivariogram of raingauge $x_i$ and raingauge $x_j$ ($mm^2$); $V_m$ is the $m$-th grid in the estimated area; $\bar{\gamma}(V_m, x_i)$ represents the average semivariogram of estimated area $V$ and raingauge $x_i$ ($mm^2$); $\lambda_i$ is the weighting of each raingauge; $\sigma_K^2$ is the Kriging estimated variance ($mm^2$); and $\mu$ denotes the Lagrange's multipliers ($mm^2$). The Kriging estimator $Z_K^*$ of the hourly mean

rainfall can be expressed as

$$Z_K^* = \sum_{i=1}^{n} \lambda_i Z(x_i) \tag{6}$$

## 3. The Model of Linear Cascade Reservoirs

The model in this study is constructed from three linear serial reservoirs with one in parallel. These reservoirs are individually viewed as independent systems by following the hydrological cycle. The inputs and outputs of linear systems are analogous to natural flows as runoff components and infiltration.

### 3.1. *Structure and flow mechanism within the model*

This model (Figure 1) has one horizontal open hole and a vertical opening in the upper and middle reservoirs in serial (Tank 1 and Tank 2), while the parallel reservoir (Tank 0) and the lowest serial reservoir (Tank 3) only have a horizontal opening. The rates at which water moves through the opening for the horizontal holes of one parallel and three serial reservoirs are denoted as $a_0$, $a_1$, $a_2$ and $a_3$, while $b_1$ and $b_2$ are for the vertical holes of the upper and middle reservoirs in serial, respectively. Flow discharges, $q_1$, $q_2$ and $q_3$, of the horizontal holes at the bottom of the three serial reservoirs are modeled as rapid subsurface, delayed

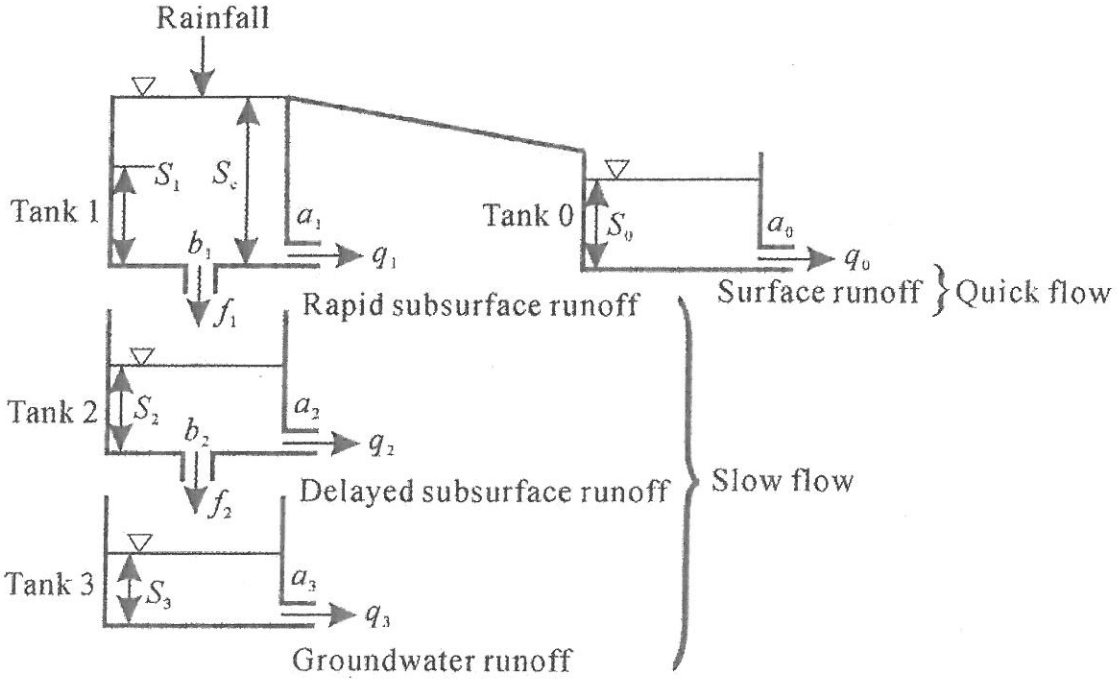


Structure of three series and one parallel cascaded linear reservoirs

Figure 1 The model structure of three serial reservoirs with one in parallel.

subsurface and groundwater runoffs. The analogous meaning of surface runoff is indicated by flow $q_0$ of a horizontal opening of the parallel reservoir when storage in the upper reservoir in serial is higher than the height $S_c$ itself. Height $S_c$ can describe the soil antecedent moisture before rainfall. Infiltration amount $f_1$ flows from a vertical hole in the upper reservoir to the middle reservoir in serial. Discharge $f_2$ represents the amount of percolation coming from the deep soil aquifer, flowing from the middle reservoir to the lowest reservoir in serial.

### 3.2. Storage functions over time

The outflows $q_1$, $q_2$, $q_3$, except surface runoff $q_0$, are expressed as follows:

$$q_i(t) = a_i S_i(t), \quad i = 1,2,3 \text{ (mm/hr)} \tag{7}$$

$$f_i(t) = b_i S_i(t), \quad i = 1,2 \text{ (mm/hr)} \tag{8}$$

The unit input of the upper reservoir in serial is the rainfall that occurred between 0 and $\Delta t$ ($\Delta t$ is 1 hour in this study), and that of the other time periods is zero. Hence, instantaneous input $I_1(t)$ equals $1/\Delta t$, and $C_1 = a_1 + b_1$; thus, storage height $S_1(t)$ of the unit input for the upper reservoir in serial can be derived as follows:

$$S_1(t) = \frac{1}{\Delta t}\frac{\left(1 - e^{-C_1 t}\right)}{C_1}, \quad 0 < t \leq \Delta t \tag{9}$$

$$S_1(t) = \frac{1}{\Delta t}\frac{\left(e^{C_1 \Delta t} - 1\right)e^{-C_1 t}}{C_1}, \quad t > \Delta t \tag{10}$$

Similarly, unit input $I_2(t)$ of the middle reservoir in serial is the infiltration output $f_1(t)$ of the upper reservoir in serial, i.e., $I_2(t) = f_1(t) = b_1 S_1(t)$, and $C_2 = a_2 + b_2$; thus, storage height $S_2(t)$ of the unit input for the middle reservoir in serial is as follows:

$$S_2(t) = \frac{1}{\Delta t}\frac{b_1}{C_1 C_2}\left[1 + \frac{C_2}{C_1 - C_2}e^{-C_1 t} - \frac{C_1}{C_1 - C_2}e^{-C_2 t}\right], \quad 0 < t < \Delta t \tag{11}$$

$$S_2(t) = \frac{1}{\Delta t}\frac{b_1}{C_1 C_2}\left[\frac{-C_2\left(e^{C_1 \Delta t} - 1\right)}{C_1 - C_2}e^{-C_1 t} + \frac{C_1\left(e^{C_2 \Delta t} - 1\right)}{C_1 - C_2}e^{-C_2 t}\right], \quad t > \Delta t \tag{12}$$

Finally, the unit input of the lowest reservoir in serial is $I_3(t) = f_2(t) = b_2 S_2(t)$, and $C_3 = a_3$; thus, storage height $S_3(t)$ of the lowest reservoir in serial

is expressed as

$$S_3(t) = \frac{1}{\Delta t}\frac{b_1 b_2}{C_1 C_2 a_3}\left[1 - \frac{C_2 a_3}{(C_1 - C_2)(C_1 - a_3)}e^{-C_1 t} + \frac{C_1 a_3}{(C_1 - C_2)(C_2 - a_3)}e^{-C_2 t} - \frac{C_1 C_2}{(C_1 - a_3)(C_2 - a_3)}e^{-a_3 t}\right], \quad 0 < t \le \Delta t \tag{13}$$

$$S_3(t) = \frac{1}{\Delta t}\frac{b_1 b_2}{C_1 C_2 a_3}\left[\frac{C_2 a_3\left(e^{C_1 \Delta t} - 1\right)}{(C_1 - C_2)(C_1 - a_3)}e^{-C_1 t} - \frac{C_1 a_3\left(e^{C_2 \Delta t} - 1\right)}{(C_1 - C_2)(C_2 - a_3)}e^{-C_2 t} - \frac{C_1 C_2\left(e^{a_3 \Delta t} - 1\right)}{(C_1 - a_3)(C_2 - a_3)}e^{-a_3 t}\right], \quad t > \Delta t \tag{14}$$

Similar to the upper reservoir in serial (Tank 1), for the unit input ($I_0 = 1$) in duration $\Delta t$, the unit pulse response function of the parallel reservoir, which is used to generate surface runoff $q_0$, can be obtained as

$$u_0(t) = \frac{1 - e^{-a_0 t}}{\Delta t}, \quad 0 < t \le \Delta t \tag{15}$$

$$u_0(t) = \frac{1}{\Delta t}(e^{a_0 \Delta t} - 1)e^{-a_0 t}, \quad t > \Delta t \tag{16}$$

### 3.3. *Parameter limitations*

Based on physical significances of the principles of the hydrological cycle, soil infiltration and runoff generation, the model parameters should be confined to the following eight limitations: (i) $a_0 > a_1$; (ii) $a_1 \ge a_2$; (iii) $a_2 > a_3$; (iv) $b_1 > b_2$; (v) $1 - (a_1 + b_1) \ge 0$; (vi) $1 - (a_2 + b_2) \ge 0$; (vii) $1 - a_3 \ge 0$; (viii) $1 - a_0 \ge 0$.

## 4. Evaluation Criteria

This study utilized three criteria to evaluate model suitability for the basin of interest. Three criteria are as follows:

(i) Coefficient of efficiency, $CE$, is defined as

$$CE = 1 - \frac{\sum_{t=1}^{T}\left[Q_{est}(t) - Q_{obs}(t)\right]^2}{\sum_{t=1}^{T}\left[Q_{obs}(t) - \bar{Q}_{obs}\right]^2} \tag{17}$$

where $Q_{est}(t)$ denotes the discharge of the simulated hydrograph for time period $t$, $Q_{obs}(t)$ is the discharge of the observed hydrograph for time period $t$, and $\bar{Q}_{obs}$ is the average discharge of the observed hydrograph. The better the fit, the closer

$CE$ is to one. A negative value for $CE$ means that model predictions are worse than predictions using a constant that is equal to the average observed value.

(ii) The error of peak discharge, $EQ_p(\%)$, is defined as

$$EQ_p(\%) = \frac{Q_{est,p} - Q_{obs,p}}{Q_{obs,p}} \times 100\% \tag{18}$$

where $Q_{est,p}$ is the peak discharge of the simulated hydrograph and $Q_{obs,p}$ is the peak discharge of the observed hydrograph.

(iii) The error of the time for peak to arrive, $ET_p$, is defined as

$$ET_p = T_{est,p} - T_{obs,p} \tag{19}$$

where $T_{est,p}$ is the time for the simulated hydrograph peak to arrive and $T_{obs,p}$ is the time required for the observed hydrograph peak to arrive.

## 5. Watershed Description

### 5.1. Geographical feature

The upstream area of the Wu-Tu Watershed was chosen to explore the characteristics of runoff components resulting from the model of three serial cascade reservoirs with a parallel reservoir. The watershed surrounds Taipei city in the northern part of Taiwan (Figure 2). The Wu-Tu Watershed covers about 204 km$^2$, and the mean annual precipitation and runoff depth are 2865 mm and 2177 mm, respectively.

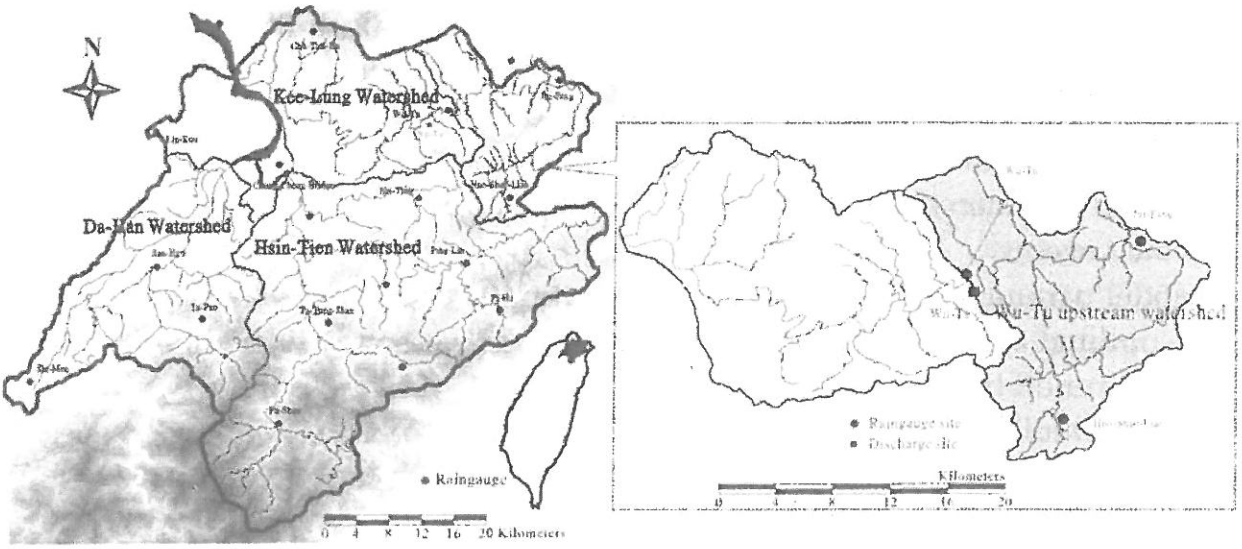


Figure 2 Location maps of the Tamshui River Basin and the Wu-Tu Watershed.

### 5.2. Rainfall-runoff material

There are three raingauges (Jui-Fang, Wu-Tu and Huo-Shao-Liao) and one discharge site (Wu-Tu) on the Wu-Tu upstream Watershed. The recorded 38 events in 1966–2008 were used as the study sample for calibration. The rainfall semivariogram was analyzed using the data from the 14 raingauges (including those at Jui-Fang, Wu-Tu and Huo-Shao-Liao) (Figure 2) located in and around the upstream portion of the Wu-Tu Watershed. Hourly mean rainfall was estimated using the block Kriging method with three raingauges (i.e., Jui-Fang, Wu-Tu and Huo-Shao-Liao) located in the Wu-Tu watershed.

## 6. Results and Discussions

This study translates rainfall into streamflow components depends on the lumped model of three serial reservoirs and one in parallel. Streamflow are divided into surface runoff, rapid and delayed subsurface runoffs, and groundwater. The quick runoff (surface runoff) and slow runoff (a sum of the subsurface and groundwater runoff) are discussed herein. Restated, this section examines the characteristics of quick and slow flows related to observations of rainfall and total runoff hydrographs. Runoff characteristics that are compared include the time to peak, peak discharge and total discharge.

### 6.1. Model calibration

The analytical results of the scaled climatological mean semivariogram for the 38 rainfall events recorded by 14 raingauges in or around the watershed were completed. The power form was then applied for fitting as follows:

$$\gamma_d^*(h_{ij}, a) = \omega_0 h^a = 0.093 h^{0.243},\ \mathrm{R}^2 = 0.906 \tag{20}$$

where $\omega_0$ denotes the scaled parameter of the scaled climatological mean semivariogram ($mm^2$). Hourly semivariograms can then be directly calculated using Eqs. (1) and (20). The estimated area was divided into 2665 × 1-$km^2$ grids for calculating hourly mean rainfall. This study used observations from three raingauges located in the Wu-Tu watershed to estimate the hourly mean rainfall for applying to the calibrated events.

Model parameters were determined by using the shuffled complex evolution (SCE) optimal algorithm.[21] Table 1 shows the comparisons of the simulated and observed runoff hydrographs using the three criteria ($CE$, $EQ_p$, and $ET_p$). Figure 3 plots two simulation results of quick and slow hydrographs in 38 calibrated events.

Regarding $CE$ for model calibration, 25 calibrated events exceed 0.8, 11 cases are within the intervals of 0.7-0.8, and only one is below 0.7 (Table 1). With regard to $EQ_p$, all samples are smaller than 20% except for six typhoons/storms. The $ET_p$ values are all less than or equal to 3 hours; three are longer than 3 hours.

The satisfactory results of model calibration using the three evaluation criteria demonstrate that the parameters are able to illustrate the situation of the watershed during rainfall-runoff processes.

## 6.2. Times to peak of hydrograph components

This study first addresses the characteristic for time to peak. An attempt is made to identify the relationships between peak time of rainfall and time to peak of

Table 1 Calibration results for the model of three serial reservoirs with one parallel reservoir.

| Event names (times) | *CE* | $EQ_p$ (%) | $ET_p$ (hrs) | Shape [a] |
|---|---|---|---|---|
| CORA (1966-09-06) | 0.95 | 15.47 | 0 | S |
| BETTY (1972-08-16) | 0.97 | −0.88 | −1 | S |
| BILLIE (1976-08-09) | 0.98 | −9.01 | 1 | S |
| VERA (1977-07-31) | 0.81 | 33.86 | 0 | S |
| ORA (1978-10-12) | 0.79 | 23.08 | −2 | M |
| IRVING (1979-08-14) | 0.94 | 18.97 | 0 | S |
| Storm (1980-11-19) | 0.87 | 18.61 | 0 | S |
| ANDY (1982-07-29) | 0.77 | 15.90 | 0 | S |
| CECIL (1982-08-09) | 0.80 | 17.71 | 0 | M |
| Storm (1983-10-12) | 0.96 | 7.54 | 1 | S |
| Storm (1983-10-14) | 0.99 | −5.74 | 0 | S |
| Storm (1984-06-02) | 0.94 | −29.21 | 0 | S |
| Storm (1984-11-18) | 0.85 | 13.01 | 2 | S |
| NELSON (1985-08-22) | 0.91 | −2.56 | 0 | S |
| ALEX (1987-07-27) | 0.88 | −5.92 | 2 | S |
| ABE (1990-08-30) | 0.76 | 11.36 | −1 | S |
| Storm (1990-09-01) | 0.92 | −4.66 | 0 | S |
| Storm (1990-09-02) | 0.92 | −16.23 | 2 | S |
| Storm (1994-06-18) | 0.85 | −16.67 | 0 | S |
| FRED (1994-08-20) | 0.93 | 15.31 | 2 | S |
| GLADYS (1994-09-01) | 0.91 | −17.05 | 2 | S |
| HERB (1996-07-31) | 0.95 | 6.23 | 1 | S |
| WINNIE (1997-08-17) | 0.79 | −2.12 | 0 | S |
| AMBER (1997-08-29) | 0.75 | 26.26 | 1 | S |
| Storm (1999-09-26) | 0.82 | −11.56 | 4 | S |
| BEBINCA (2000-11-08) | 0.68 | 12.79 | 0 | M |
| RANANIM (2004-08-12) | 0.61 | −8.16 | 1 | M |
| Storm (2004-08-17) | 0.87 | −13.36 | 2 | S |
| Storm (2004-10-01) | 0.79 | 12.78 | 2 | S |
| Storm (2005-05-09) | 0.78 | 26.76 | 1 | S |
| Storm (2005-09-10) | 0.76 | −4.62 | 3 | S |
| Storm (2005-12-04) | 0.88 | 1.44 | 3 | S |
| Storm (2005-12-11) | 0.70 | 17.90 | 5 | S |
| Storm (2006-06-06) | 0.85 | 10.57 | 4 | M |
| Storm (2007-06-15) | 0.94 | −28.79 | 1 | S |
| Storm (2007-09-04) | 0.94 | −18.36 | 1 | S |
| Storm (2008-05-30) | 0.72 | −13.62 | 1 | S |
| Storm (2008-10-10) | 0.87 | 8.55 | 1 | S |

[a] The S notation represents a single-peak event, and the M notation represents a multi-peak event.

runoff components. Figures 4a and b plot the correlations between peak times of hyetographs and both hydrograph components, respectively. These positive correlations, excluding multi-peak rainfall-runoff events, are between peak rainfall for slow runoffs and peak rainfall for quick runoffs. These figures also reveals that the power relationship for peak time between rainfall and quick runoff ($R^2$ = 0.63) is more obvious than between rainfall and slow runoff ($R^2$ = 0.47). The established relationship of rainfall to quick runoff is markedly higher than that of rainfall to slow runoff. This is because slow water flowing beneath land surface is influenced not only by infiltration resulting from rainfall, but also by porosity, soil moisture and hydraulic conductivity of the soil layers. The above analytical results demonstrate that time to peak of a quick flow is highly correlated with peak time of a hyetograph and a slow flow has also a visual correlation with rainfall.

Based on the above results, this study concludes that time to peak of a slow runoff is later than that of a quick runoff. Moreover, the times to peak of both component hydrographs are related to peak time of rainfall, and their relationships are power form except for the multi-peak events.

### 6.3. *Peak discharges of hydrograph components*

This study also analyzes the relationships between hydrograph components and observed total runoffs in terms of peak discharges. The above analytical findings indicate that a large total runoff hydrograph (a sum of quick, slow runoffs and baseflow) has a large peak for quick runoff, and is larger than that of a slow runoff.

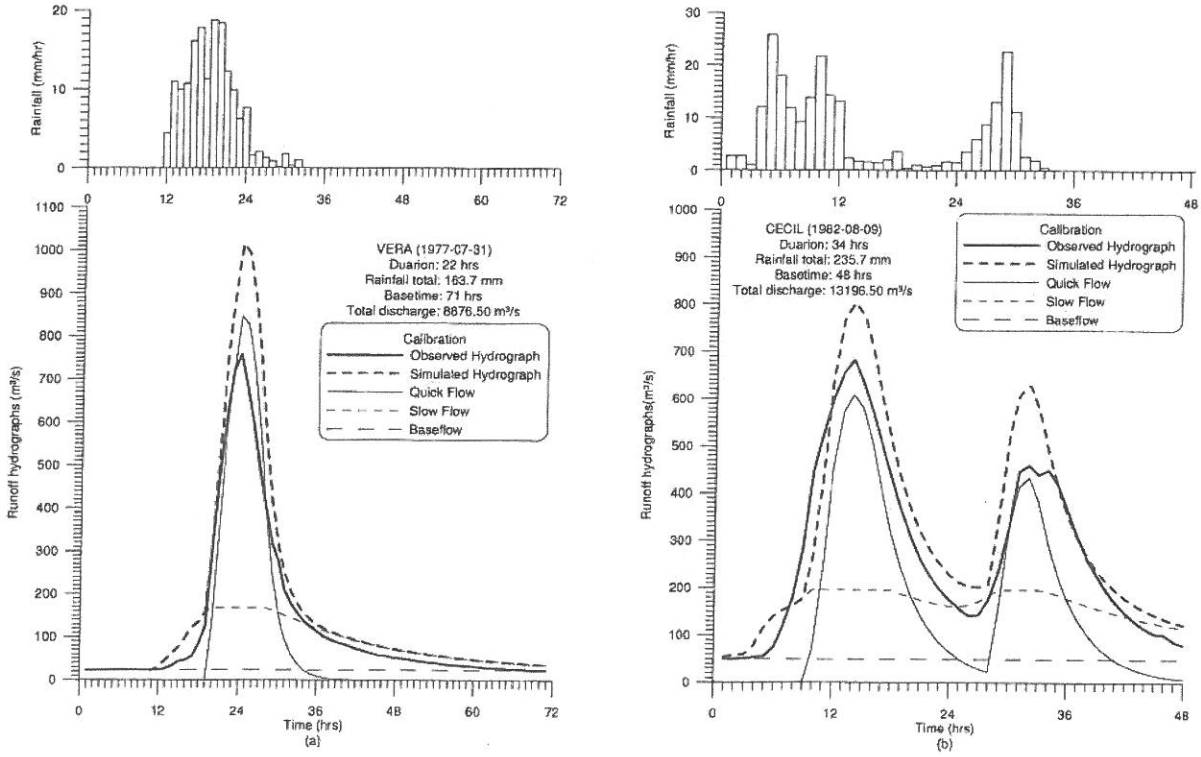


Figure 3 Calibrations of runoff hydrographs for rainfall-runoff events.

Figure 5 plots the obvious relationships for peak discharges between component hydrographs and observations of total runoffs. Two linear relationships are evident according to $R^2$ values, i.e., $R^2 = 0.93$ and $R^2 = 0.58$ for simulated quick and slow runoffs to total runoff observations, respectively. The extent of correlation for quick runoff with total runoff is stronger than that of slow runoff with total runoff because slow runoff movements in an aquifer are more complex than surface runoff (quick runoff) that runs on the ground surface. Figure 5 further indicates that, while peak discharges of quick runoffs are slightly smaller than those of observed total runoff, peaks of slow runoffs are significantly smaller than those of observed total runoffs. With respect to multi-peak and single-peak cases, the ratios are 1-0.83 for observed total runoffs to surface (quick) runoffs and 1-0.17 for observed total runoffs to slow runoffs.

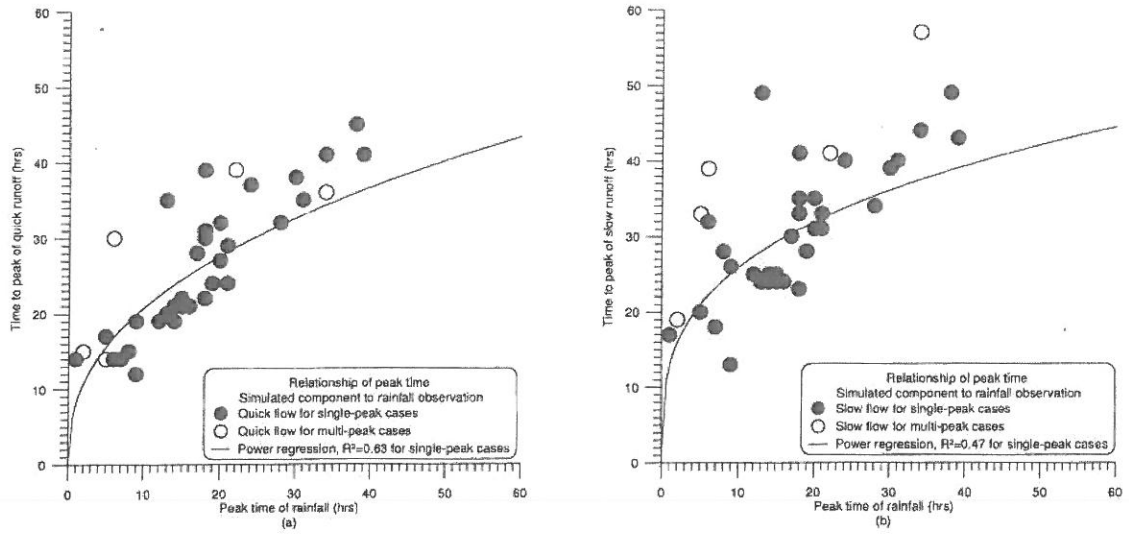


Figure 4 The relationships of peak times between simulated hydrograph components and rainfall observation.

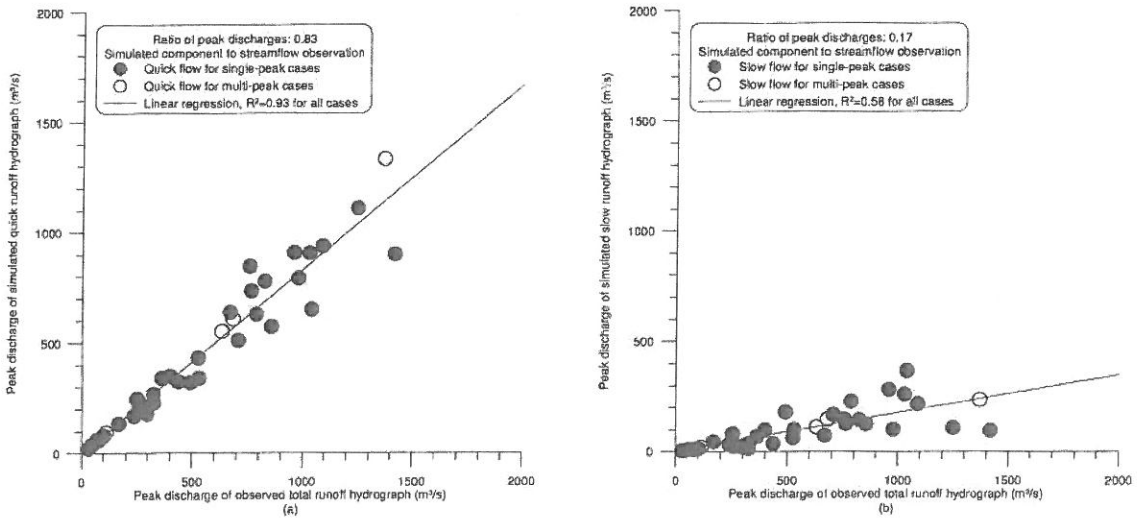


Figure 5 The relationships of peak discharges between simulated hydrograph components and observed total runoffs.

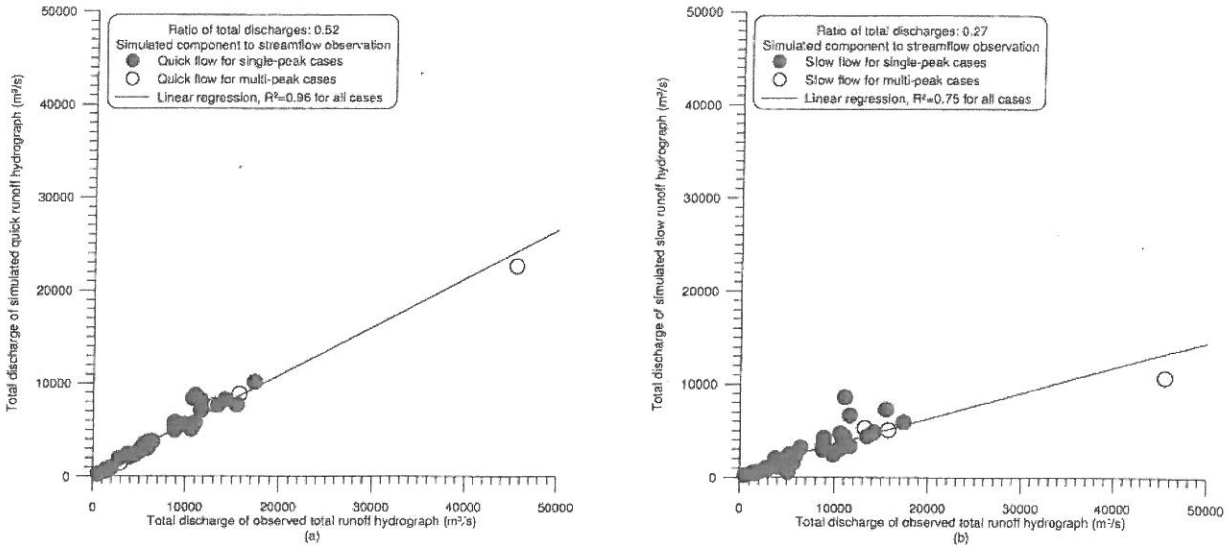


Figure 6 The relationships of total discharges between simulated hydrograph components and observed total runoffs.

### 6.4. *Total discharges of hydrograph components*

Finally, this study discusses the final characteristic of hydrograph components. Figure 6 plots the comparison results of individual components to observed total runoff for further identifying the ratio percentages of component flows during rainfall-runoff episodes. For the same events, the points representing specific values for total discharges of surface (quick) runoffs to those of total runoffs (Figure 6a) are above those resulting from ratios of slow runoffs to total runoffs (Figure 6b). According to Figs. 6a and b, volume of quick flows is larger than that of slow flows in rainfall-runoff generations. Both variations of roughly straight lines can be found for percentages of quick flows to total flows ($R^2 = 0.96$) and slow flows to total flows ($R^2 = 0.75$). Regardless of multi-peak or single-peak rainfall-runoff events, the volume of a surface runoff is 52% volume of the total runoff and 27% for that of a slow runoff; whereas the remainder is baseflow components.

## 7. Conclusions

This study used a model of three serial reservoirs with one parallel reservoir and limited seven significant parameters to simulate runoff components in a river outlet. Based on the calibration results, seven parameters were established and offer effective assistance on observing runoff components in streamflows of a watershed outlet. The regenerated results show this model is suitable to evaluate hydrological conditions in this and other watersheds and to apply it further to watershed management in Taiwan.

Based on the results of this study, the following significant findings are described: (i) The times to peak for both hydrograph components of single-peak

events is an increasing power correlation corresponding to peak time of a hyetograph; (ii) For all events, the ratio of a quick runoff to the observed total runoff is linearly approximately 83% and 17% for a slow flow to observations of the same total runoff; and (iii) For all events, total discharge of a quick runoff component is a direct ratio of 52% that of a total runoff and 27% of that for a slow runoff. The remainder is baseflow in the same total flow. When given rainfall conditions and total runoff hydrographs, analytical results of this study significantly contribute to efforts to evaluate hydrograph characteristics of quick and slow runoffs and, thus provide a valuable reference for watershed management in Taiwan.

## References


1. J. E. Nash, The form of the instantaneous unit hydrograph, *IAHS Publications* **45**, 112–121 (1957).
2. M. M. Ahmad, A. R. Ghumman and S. Ahmad, Estimation of Clark's instantaneous unit hydrograph parameters and development of direct surface runoff hydrograph, *Water Resour. Manag.* **23**, 2417–2435 (2009).
3. V. Nourani, V. P. Singh and H. Delafrouz, Three geomorphological rainfall-runoff models based on the linear reservoir concept, *Catena* **76**, 206–214 (2009).
4. L. S. Hsieh and R. Y. Wang, A semi-distributed parallel-type linear reservoir rainfall-runoff model and its application in Taiwan, *Hydrol. Process.* **13**, 1247–1268 (1999).
5. U. Agirre, M. Goñi, J. J. López and F. N. Gimena, Application of a unit hydrograph based on subwatershed division and comparison with Nash's instantaneous unit hydrograph, *Catena* **64**, 321–332 (2005).
6. F. Melone, C. Corradini and V. P. Singh, Simulation of the direct runoff hydrograph at basin outlet, *Hydrol. Process.* **12**, 769–779 (1998).
7. A. Bhadra, A. Bandyopadhyay, R. Singh and N. S. Raghuwanshi, Rainfall-runoff modeling: comparison of two approaches with different data requirements, *Water Resour. Manag.* **24**, 37–62 (2010).
8. S. J. Cheng and R. Y. Wang, An approach for evaluating the hydrological effects of urbanization and its application, *Hydrol. Process.* **16**, 1403–1418 (2002).
9. S. J. Cheng, H. H. Hsieh, C. F. Lee and Y. M. Wang, The storage potential of different surface coverings for various scale storms on Wu-Tu Watershed, Taiwan, *Nat. Hazards* **44**, 129–146 (2008b).
10. H. J. Huang, S. J. Cheng, J. C. Wen and J. H. Lee, Effect of growing watershed imperviousness on hydrograph parameters and peak discharge, *Hydrol. Process.* **22**, 2075–2085 (2008a).
11. S. Y. Huang, S. J. Cheng, J. C. Wen and J. H. Lee, Identifying peak- imperviousness-recurrence relationships on a growing-impervious watershed, Taiwan, *J. Hydrol.* **362**, 320–336 (2008b).
12. S. J. Cheng, C. F. Lee and J. H. Lee, Effects of urbanization factors on model parameters, *Water Resour. Manag.* **24**, 775–794 (2010).
13. A. J. Jakeman, I. G. Littlewood and P. G. Whitehead, Computation of the instantaneous unit hydrograph and identifiable component flows with application to two upland catchments, *J. Hydrol.* **117**, 275–300 (1990).
14. A. J. Jakeman and G. M. Hornberger, How much complexity is warranted in a rainfall-runoff model? *Water Resour. Res.* **29**, 2637–2649 (1993).

15. M. Sugawara, Automatic calibration of the tank model, *Hydrolog. Sci. Bull.* **24**, 375–388 (1979).
16. M. Sugawara, 'Tank model', in *Computer Models of Watershed Hydrology*, ed. V. P. Singh (Water Resources Publications, Littleton, Colorado 1995), pp. 165–214.
17. M. Hashino, H. Yao and H. Yoshida, Studies and evaluations on interception processes during rainfall based on a tank model, *J. Hydrol.* **255**, 1–11 (2002).
18. Y. H. Lee and V. P. Singh, Tank model for sediment yield, *Water Resour. Manag.* **19**, 349–362 (2005).
19. G. Bastin, B. Lorent, C. Duque and M. Gevers, Optimal estimation of the average rainfall and optimal selection of raingauge locations, *Water Resour. Res.* **20**, 463–470 (1984).
20. S. J. Cheng, H. H. Hsieh and Y. M. Wang, Geostatistical interpolation of space-time rainfall on Tamshui River Basin, Taiwan, *Hydrol. Process.* **21**, 3136–3145 (2007).
21. Q. Duan, V. K. Gupta and S. Sorooshian, Shuffled complex evolution approach for effective and efficient global minimization, *J. Optim. Theory Appl.* 76, 501–521 (1993).